CHEMISTRY
A EUROPEAN JOURNAL

DOI: 10.1002/chem.200500603

A Close Look at Short C–CH_3···Potassium Contacts: Synthetic and Theoretical Investigations of $[M_2Co_2(\mu_3\text{-}OtBu)_2(\mu_2\text{-}OtBu)_4(thf)_n]$ (M = Na, K, Rb, thf = tetrahydrofuran)

Christopher E. Anson,[a] Wim Klopper,*[b] Jin-Shan Li,[a] Lukasz Ponikiewski,[a] and Alexander Rothenberger*[a, c]

Abstract: Agostic interactions of the type Si–CH_3···M^+ (M = alkali metal) are frequently mentioned in discussions of solid-state structures of trimethylsilyl compounds and the purpose of this work was to elucidate if they also exist in the related *tert*-butyl species by using density functional theory. The compounds $[M_2Co_2(\mu_3\text{-}OtBu)_2(\mu_2\text{-}OtBu)_4(thf)_n]$ (M = Na, $n = 2$; M = K, $n = 0$; M = Rb, $n = 1$) have been synthesised and their crystal structures determined. Close contacts of methyl groups with K atoms are observed in the solid-state structure of $[K_2Co_2(\mu_3\text{-}OtBu)_2(\mu_2\text{-}OtBu)_4]$, and calculations of the rotational barrier of a *tert*-butoxy group about the axis through the C–O bond were performed. It was shown that apparent short C–CH_3···K distances are in this case a consequence of the packing in the extended solid-state structure.

Keywords: agostic interactions · alkali metals · density functional calculations · metal alkoxides

Introduction

The incorporation of cobalt into elaborate inorganic architectures is an active area of research due to the interest in magnetic materials.[1] The starting materials used in these investigations are often Co^{II} halides. Cobalt alkoxides represent alternative Co-containing starting materials for these investigations, with the advantage of their solubility in organic solvents. The preparation of cobalt alkoxides is straightforward and the synthesis of a range of homoleptic Co^{II} alkoxides containing bulky organic substituents was achieved by alcoholysis reactions of $Co(NSiMe_3)_2$.[2,3] A different method commonly used for the preparation of alkoxides are metathesis reactions.[4] The reactions of Co^{II} halides and alkali metal alkoxides, however, give heterometallic alkoxides of the general formula $[M_2Co_2(\mu_3\text{-}OtBu)_2(\mu_2\text{-}OtBu)_4]$ (M = alkali metal).[5] The alkali metal atoms in these Co^{II} complexes are coordinated by etheral solvent molecules.[5] In the absence of donor solvents (e.g., ethers, amines), alkali metal atoms in general can undergo cation–π interactions with aromatic solvents or be stabilized by what is sometimes described as agostic interactions.[6–9] In contrast to the classical agostic M···H–C bonds in transition metals which are well-understood,[10] C–CH_3···alkali metal interactions are difficult to quantify and it is not clear if they exist at all. As a contribution to this area we report here the synthesis of a series of Co^{II} complexes and describe a DFT case study on C–CH_3···K^+ interactions in $[K_2Co_2(\mu_3\text{-}OtBu)_2(\mu_2\text{-}OtBu)_4]$.

[a] Dr. C. E. Anson, Prof. J.-S. Li, L. Ponikiewski, Dr. A. Rothenberger
Institut für Anorganische Chemie, Universität Karlsruhe (TH)
Engesserstrasse 15, 76131 Karlsruhe (Germany)
E-mail: ar252@chemie.uni-karlsruhe.de

[b] Prof. Dr. W. Klopper
Institut für Physikalische Chemie, Universität Karlsruhe (TH)
Fritz-Haber-Weg 4, 76131 Karlsruhe (Germany)
E-mail: klopper@chem-bio.uni-karlsruhe.de

[c] Dr. A. Rothenberger
Institut für Nanotechnologie
Forschungszentrum Karlsruhe GmbH
Postfach 3640, 76021 Karlsruhe (Germany)

Supporting information for this article is available on the WWW under http://www.chemeurj.org/ or from the author.

Results and Discussion

As part of a project to investigate the reactivity of heterometallic alkoxides we prepared a series of Co/alkali metal alkoxide starting materials of the type $[M_2Co_2(\mu_3\text{-}OtBu)_2(\mu_2\text{-}OtBu)_4(thf)_n]$ (M = Na, K, Rb).[11] The synthetic approach to the complexes involved the reactions of three equivalents of M*O*t*Bu* (M = Na, K, Rb) with $CoBr_2$ in thf at ambient tem-

perature (Scheme 1). Removal of the solvent and recrystallisation of the solid blue residues from pentane produced $[Na_2Co_2(\mu_3\text{-}OtBu)_2(\mu_2\text{-}OtBu)_4(thf)_2]$ (**1**), $[K_2Co_2(\mu_3\text{-}OtBu)_2(\mu_2\text{-}OtBu)_4]$ (**2**) and $[Rb_2Co_2(\mu_3\text{-}OtBu)_2(\mu_2\text{-}OtBu)_4(thf)]$ (**3**) in good yield.

$$6MO\mathit{t}Bu + 2CoBr_2 \xrightarrow[\text{pentane}]{\text{thf}} [(thf)_xM\{Co(O\mathit{t}Bu)_3\}]_2 + 4MBr \quad \begin{matrix} M=Na,\ x=1 & (\mathbf{1}) \\ K \quad 0 & (\mathbf{2}) \\ Rb \quad 0.5 & (\mathbf{3}) \end{matrix}$$

Scheme 1. Synthesis of **1**–**3**.

An X-ray crystallographic study of **1**–**3** revealed that all complexes consist of a central $[M_2Co_2(\mu_3\text{-}OtBu)_2(\mu_2\text{-}OtBu)_4]$ core. The structure of **1** is shown in Figure 1.

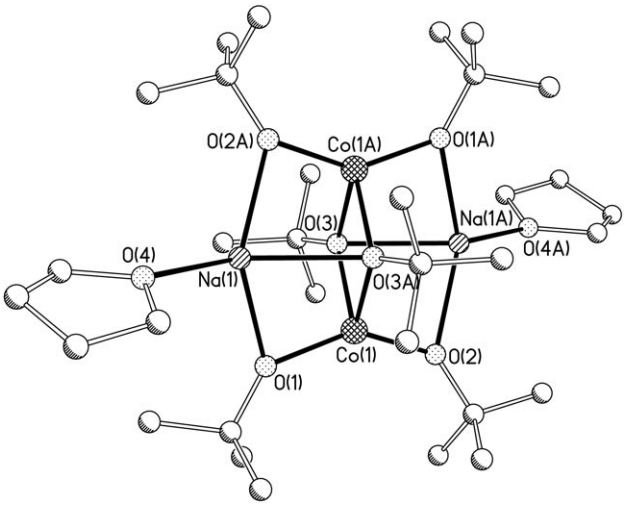

Figure 1. Structure of **1** in the solid state (hydrogen atoms have been omitted for clarity). Symmetry transformation: A = $-x$, $-y$, $-z+1$. Selected bond lengths [Å] and angles [°]: Na(1)–O(1) 2.2883(15), Na(1)–O(2A) 2.2885(15), Na(1)–O(4) 2.3366(17), Na(1)–O(3A) 2.4258(14), Co(1)–O(2) 1.8926(13), Co(1)–O(1) 1.9001(13), Co(1)–O(3A) 2.0043(12), Co(1)–O(3) 2.0297(11), Co(1)–Na(1A) 3.0282(9); O(1)-Na(1)-O(2 A) 133.48(6), O(1)-Na(1)-O(4) 108.95(6), O(2A)-Na(1)-O(4) 116.66(6), O(1)-Na(1)-O(3A) 76.25(5), O(2A)-Na(1)-O(3A) 75.62(5), O(4)-Na(1)-O(3A) 138.88(7), O(2)-Co(1)-O(1) 144.69(6), O(2)-Co(1)-O-(3 A) 112.40(5), O(1)-Co(1)-O(3 A) 96.44(5), O(2)-Co(1)-O(3) 94.95(5), O(1)-Co(1)-O(3) 109.65(6), O(3A)-Co(1)-O(3) 81.39(5), Co(1)-O(1)-Na(1) 92.05(5), Co(1)-O(2)-Na(1A) 92.33(5), Co(1 A)-O(3)-Co(1) 98.61(5), Co(1A)-O(3)-Na(1A) 85.61(5), Co(1)-O(3)-Na(1A) 85.14(4).

The size of the alkali metal ion in **1**–**3** has little influence on the bond lengths and angles within the $[Co_2(OtBu)_6]$ units in **1**–**3**. The dimeric $[M_2Co_2(\mu_3\text{-}OtBu)_2(\mu_2\text{-}OtBu)_4]$ units form a centrosymmetric arrangement in which the Co atoms are tetrahedrally coordinated by two μ_2- and two μ_3-*tert*-butoxy groups. The exterior O-Co-O angles O(2)-Co(1)-O(1) 144.69(6) (**1**), O(2A)-Co(1)-O(3) 135.55(7) (**2**) and O(3)-Co(1)-O(1) 132.56(18) (**3**) are the largest change observed in the $[Co_2(\mu_3\text{-}OtBu)_2(\mu_2\text{-}OtBu)_4]$ frameworks of **1**–**3**. The M–O*t*Bu bond lengths increase with the size of the alkali metal atom (av M–O 2.3 (**1**), 2.5 (**2**), 2.8 Å (**3**)). Similar structural motifs were observed in the closely related heterometallic transition-metal alkoxides $[K_2Zn_2(\mu_3\text{-}OtBu)_2(\mu_2\text{-}OtBu)_4]$ and $[Na_2Fe_2(\mu_3\text{-}OtBu)_2(\mu_2\text{-}OtBu)_4(thf)_2]$.[12,13]

In **1**, both of the Na^+ ions are additionally ligated by thf molecules, which could not be removed even by exposing the solid to dynamic vacuum. In compound **3**, however, only one of the Rb^+ ions is ligated by a thf molecule (Figure 2).

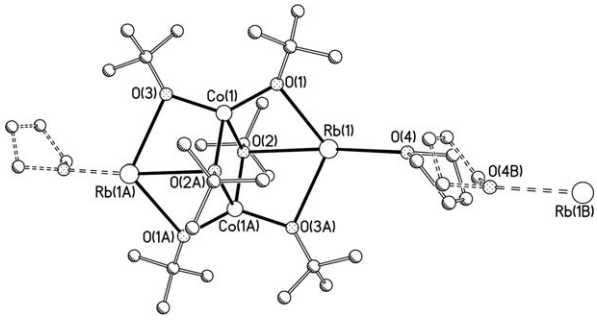

Figure 2. Structure of **3** in the solid state. Symmetry transformation: A = $-x-2$, $-y-1$, $-z-2$. Selected bond lengths [Å] and angles [°]: Rb(1)–O(1) 2.746(5), Rb(1)–O(3A) 2.756(4), Rb(1)–O(4) 2.870(15), Rb(1)–O(2) 2.894(4), Co(1)–O(3) 1.911(5), Co(1)–O(1) 1.917(5), Co(1)–O(2A) 2.025(3), Co(1)–O(2) 2.030(3); O(1)-Rb(1)-O(3 A) 114.95(15), O(1)-Rb(1)-O(4) 108.8(4), O(3A)-Rb(1)-O(4) 108.2(4), O(1)-Rb(1)-O(2) 65.00(11), O(3A)-Rb(1)-O(2) 64.45(11), O(4)-Rb(1)-O(2) 163.5(4), O(3)-Co(1)-O(1) 132.56(18), O(3)-Co(1)-O(2 A) 99.96(19), O(1)-Co(1)-O(2A) 115.89(17), O(3)-Co(1)-O(2) 116.09(16), O(1)-Co(1)-O(2) 100.40(19), O(2A)-Co(1)-O(2) 80.30(14), Co(1A)-O(2)-Co(1) 99.70(14), Co(1A)-O(2)-Rb(1) 89.78(12), Co(1)-O(2)-Rb(1) 89.36(12).

In the crystal structure of **3**, the $[Rb_2Co_2(\mu_3\text{-}OtBu)_2(\mu_2\text{-}OtBu)_4]$ units form infinite chains and the thf molecules are situated between adjacent pairs of complex units, disordered over an inversion centre. Within each chain, the molecules are presumed to be largely ordered, arranged such that each uncoordinated Rb^+ ion faces the $-C_2H_4-$ moiety of a thf ligand coordinated to a Rb^+ ion in the next molecule.

Despite repeated attempts we were unable to obtain the Na and Rb complexes **1** and **3** solvent-free as single crystalline material. Having characterized the cobalt complexes $[Na_2Co_2(\mu_3\text{-}OtBu)_2(\mu_2\text{-}OtBu)_4(thf)_2]$ (**1**), $[K_2Co_2(\mu_3\text{-}OtBu)_2(\mu_2\text{-}OtBu)_4]$ (**2**), and $[Rb_2Co_2(\mu_3\text{-}OtBu)_2(\mu_2\text{-}OtBu)_4(thf)]$ (**3**) our attention now focussed on **2**, in which the potassium atoms are solely coordinated by O atoms of *tert*-butoxy ligands and surrounded by *t*Bu groups of adjacent molecules, with no additional ligation by thf. The $[K_2Co_2(\mu_3\text{-}OtBu)_2(\mu_2\text{-}OtBu)_4]$ units form a one-dimensional polymeric arrangement in which *tert*-butoxy ligands of adjacent $[Co_2(\mu_3\text{-}OtBu)_2(\mu_2\text{-}OtBu)_4]^{2-}$ ion units form cavities containing potassium ions (Figure 3). Since these appeared to involve close C–H··K contacts, the positions of all the hydrogen atoms in **2** were refined in the structure. This refinement readily yielded satisfactory tetrahedral geometries around the methyl carbon atoms.

A closer look at the environment of the K atoms in **2** is presented in Figure 4 and shows that up to eight of the K···H distances in **2** (Table 1) are within the range of agostic

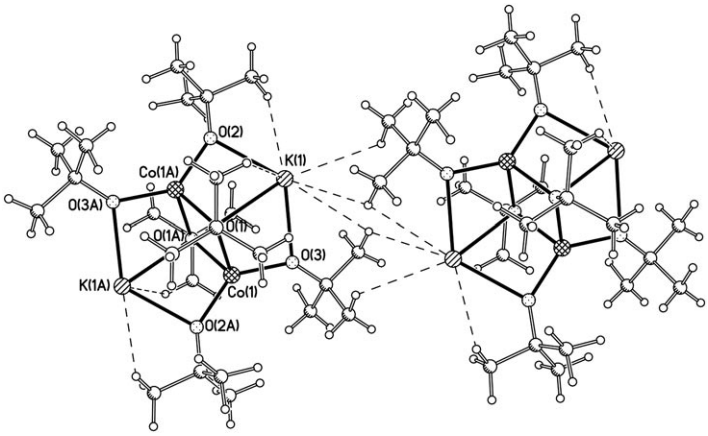

Figure 3. Structure of two molecules of **2** in the solid state. Symmetry transformation: A = $-x+1$, $-y+1$, $-z+1$. Selected bond lengths [Å] and angles [°]: Co(1)–O(2A) 1.9004(14), Co(1)–O(3) 1.9079(14), Co(1)–O(1A) 2.0233(13), Co(1)–O(1) 2.0239(14), K(1)–O(2) 2.5796(17), K(1)–O(3) 2.5948(17), K(1)–O(1) 2.7337(14); O(2A)-Co(1)-O(3) 135.55(7), O(2A)-Co(1)-O(1A) 99.05(6), O(3)-Co(1)-O(1A) 114.31(6), O(2A)-Co(1)-O(1) 115.47(6), O(3)-Co(1)-O(1) 99.11(6), O(1A)-Co(1)-O(1) 80.18(6), O(2)-K(1)-O(3) 122.50(5), O(2)-K(1)-O(1) 68.31(4), O(3)-K(1)-O(1) 68.29(5), Co(1A)-O(1)-Co(1) 99.82(6), Co(1A)-O(1)-K(1) 87.21(4), Co(1)-O(1)-K(1) 87.80(5).

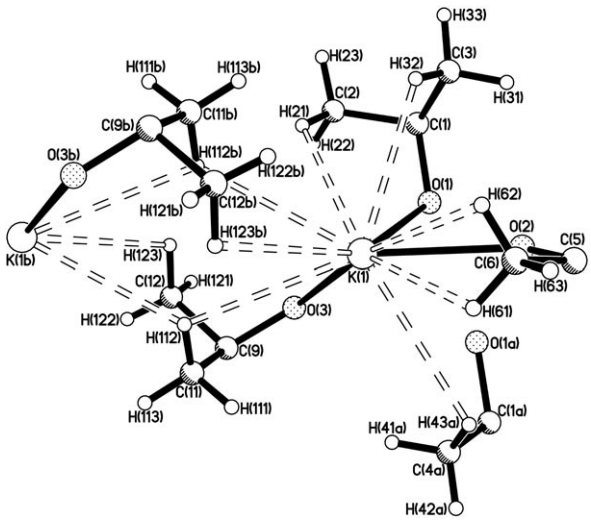

Figure 4. Coordination environment of the K atoms in two molecules of **2**. Symmetry labels: a = $-x+1$, $-y+1$, $-z+1$; b = $-x+1$, $-y$, $-z+1$. See also Table 2.

Table 1. List of experimental (solid state of **2**) and calculated (dimer of **2**) C···K, H···K distances [Å] and C–H···K angles [°] in two molecules of **2**.

	C···K		H···K		C–H···K	
	exptl	calcd	exptl	calcd	exptl	calcd
C(2)–H(21)···K(1)	3.786(3)	3.78	3.14(3)	3.16	123(2)	116
C(3)–H(32)···K(1)	3.677(3)	3.79	3.08(3)	3.16	120(2)	117
C(4a)–H(43a)···K(1)	3.802(3)	3.82	3.32(3)	3.31	112(2)	110
C(6)–H(61)···K(1)	3.413(3)	3.51	2.99(5)	3.21	109(3)	97
C(6)–H(62)···K(1)	3.413(3)	3.51	3.10(5)	3.21	101(3)	97
C(11)–H(112)···K(1)	3.588(3)	3.66	3.19(4)	3.23	106(2)	105
C(11)–H(112)···K(1b)	3.640(3)	3.79	3.07(4)	3.16	116(3)	118
C(C12b)–H(121b)···K(1)	3.631(3)	3.82	4.38(5)	4.74	32(2)	28
C(C12b)–H(122b)···K(1)	3.631(3)	3.82	3.42(5)	3.48	96(4)	100
C(C12b)–H(123b)···K(1)	3.631(3)	3.82	3.13(4)	3.26	119(3)	113

interactions (commonly discussed close Si–CH_3···alkali metal contacts of about 3 Å are observed in solid-state structures).[6,7,14] Similar short C–CH_3···K (instead of Si–CH_3···alkali metal) contacts are present in **2**. Five of these can be described as intramolecular, while one is intermolecular. More intriguingly, the remaining two close contacts, those involving H(112) and its symmetry equivalent, apparently constitute the first example of a bridging agostic interaction between two M^+ ions. This prompted us to investigate their nature and evaluate possible interactions using DFT methods (Figure 4, Table 2).

Table 2. List of calculated H···K distances [Å] in two molecules of **2** after rotation of an angle α about the C(9)–O(3) bond.

α	H(112)–K(1b)	H(121)–K(1b)	H(122)–K(1b)	H(123)–K(1b)
0	3.16	4.74	3.48	3.26
10	3.46	4.41	3.22	2.99
20	3.79	4.07	2.99	2.79
30	4.13	3.73	2.80	2.66
40	4.47	3.40	2.65	2.64
50	4.80	3.09	2.57	2.71
60	5.11	2.83	2.56	2.88

Ab initio calculations: In the crystal structure of [$K_2Co_2(\mu_3$-O*t*Bu$)_2(\mu_2$-O*t*Bu$)_4$] (**2**), the positions of the hydrogen atoms were all freely refined. To investigate the nature of the C–CH_3···K contacts, which could either be weak electrostatic or simply the result of crystal packing, density-functional theory (DFT) calculations using the TURBOMOLE program were performed at various levels (using the functionals BP86, B3LYP and TPSS with the basis sets SV(P), TZVP and TZVPP).[15] In the following, we shall discuss the results of the calculations with the TPSS functional in the TZVPP basis, which we regard as the most reliable. First, the geometry of the dimer of **2** was optimised. In this optimised geometry, of course, the *tert*-butoxy group that is coordinated with O(3) to Co(1) adopts its energetically most favourable position. Second, the energy profile was computed for rotation of this *tert*-butoxy group about the axis through its C(9)–O(3) bond. The rotation was performed in such a manner that the methyl group with carbon atom C(11) moved away from the potassium atom K(1b). Accordingly, the K(1b)–H(112) distance increased from 3.16 Å to 5.11 Å on rotation from 0° to 60° (Table 2).

At the same time, the methyl group with the carbon atom C(12) moved towards K(1b). While the -O*t*Bu group acts as a bidentate ligand with its C(11) and C(12) methyl groups at 0°, it becomes a monodentate ligand after rotation by about 60°, with only the C(12) methyl group pointing towards the potassium atom K(1b). In this rotated ge-

ometry, the three H atoms of the methyl group are rather close to K(1b), at distances of 2.83 Å, 2.56 Å and 2.88 Å (cf. Table 2). Rotating further from 60° to 120° approximately rotates back the *tert*-butoxy group into its original position (not exactly, because there is no exact local C_3 axis). It was therefore sufficient to investigate the rotation from 0° to 120°, from a bidentate via a monodentate back to a bidentate *tert*-butoxy group. The results of these calculations are depicted by the curve with a solid line in Figure 5.

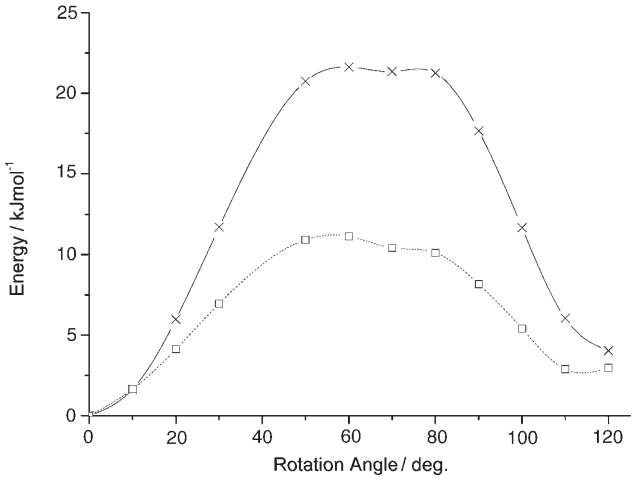

Figure 5. Energy profile for the barrier to rotation of the -O*t*Bu group in one monomer of the dimer of **2** about its C–O bond.

First, we observe that the structure at 0° is indeed a minimal-energy structure, and that a very similar structure (only ca. 4.0 kJ mol^{-1} above the minimum) is obtained after rotation by about 120°. The energy profile shows a plateau at 50–80°, at which one of the methyl groups points toward the potassium atom of the neighbouring monomer at a rather short distance (2.56–2.88 Å). The maximum at about 60° is found to be about 21.6 kJ mol^{-1} above the minimum. Thus, we conclude that there is a repulsive interaction after rotating the -O*t*Bu group by about 60°. To quantify this repulsive interaction more accurately, one has to compare the computed energy profile of the barrier to rotation about the C(9)–O(3) bond in the dimer of **2** with the energy profile that one would obtain in the monomer **2** alone, without neighbour. Corresponding calculations of the monomer (but in the geometry of the optimised dimer using all of the dimer TZVPP basis functions, that is, in the framework of a full counterpoise calculation) yielded the dashed curve in Figure 5. Except for the height of the barrier, the energy profile of the monomer is almost identical with that of the dimer. Most importantly, the optimal angle in the dimer is the same as in the monomer. Thus, in the dimer, the neighbouring cluster has no effect on the orientation of -O*t*Bu group. In the monomer, the barrier to rotation has its maximum also at about 60°, but it is not as high as in the dimer. From this, we conclude that the barrier in the dimer is higher by roughly 10 kJ mol^{-1} due to steric hindrance of the methyl group by the neighbouring cluster, that is, the potassium atom. Indeed, the binding energy of the dimer with respect to dissociation into two isolated monomers amounts to 11.7 kJ mol^{-1} at the counterpoise corrected TPSS/TZVPP level, which is reduced to only 1.1 kJ mol^{-1} after rotation of the -O*t*Bu group by about 60°. All of the calculations were repeated with ethoxy ligands in place of *tert*-butoxy ligands—giving a compound that we have so far failed to synthesize—and similar profiles of the barriers to rotation were obtained for both monomer and dimer. In fact, the energy profiles of the barriers to rotation were identical for the $[K_2Co_2(\mu_3\text{-}OEt)_2(\mu_2\text{-}OEt)_4]$ cluster and its dimer, except that the energy profile of the dimer showed an extra barrier (at about 130–140°, cf. Figure 6) due to the strong steric hindrance between the ethoxy group that was rotated and an ethoxy group of the neighbouring cluster. No C–CH_3···potassium interactions were found in this compound.

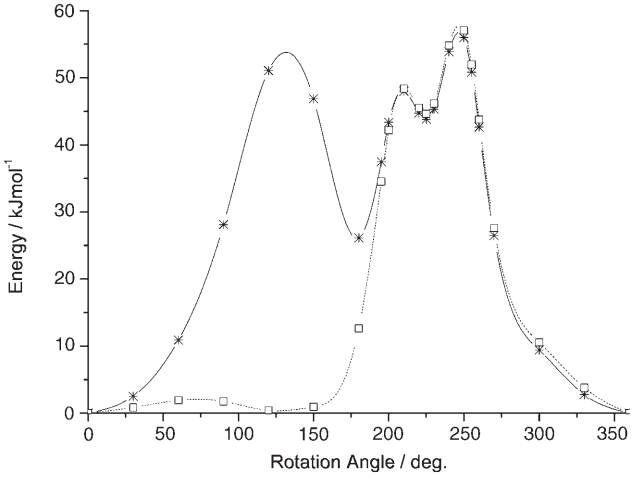

Figure 6. Energy profile for the barrier to rotation of the -OEt group in one monomer of the dimer of the virtual compound $K_2[Co_2(OEt)_6]$ about its C–O bond.

Since the computed barriers to rotation did not support a type of C–CH_3···K interaction that we would dare to characterise as an agostic interaction, we decided to compute atomic charges and bond orders to obtain insight into the bonding electron density of the C–CH_3···K moiety. With the TURBOMOLE program, we computed the Mulliken and Roby–Davidson atomic charges as implemented by Ehrhardt and Ahlrichs,[16,17] and with the Gaussian 03 and NBO 5.G programs, we computed natural populations, Wiberg bond orders (Wiberg bond indices) and atom–atom overlap weighted NAO bond orders in the framework of a natural bond order (NBO) analysis.[18,19] The TPSS functional was used with both programs, but the TZVPP basis was used with TURBOMOLE and the 6–31G** basis with Gaussian 03. All calculations were single-point calculations of the TPSS/TZVPP-optimised structure of the dimer of **2**, and the relevant C–C and C–H distances of the C–CH_3···K moiety in this structure are given in Table 3 (cf. Figure 4).

Table 3. List of calculated C–C and C–H distances [Å] in two molecules of **2** (TPSS/TZVPP level).

	Distance [Å]		Distance [Å]
C(9)–C(11)	1.544	C(9)–C(12)	1.544
C(11)–H(111)	1.095	C(11)–H(112)	1.099
C(11)–H(113)	1.098	C(12)–H(121)	1.093
C(12)–H(122)	1.098	C(12)–H(123)	1.097

We observe in Table 3 that we can distinguish between two classes of C–H bonds. Bonds in the range 1.097–1.099 Å are observed for the C–H bonds that are directed towards the K atom, and shorter bonds of 1.093–1.095 Å are found for the remaining C–H bonds. Although the C(11)–H(112) distance (1.099 Å) is the longest C–H distance, even though H(112) is the H atom closest to K(1b), it is only 0.001–0.002 Å longer than three other C–H bonds. Mulliken and Roby–Davidson atomic charges are displayed in Table 4 for the dimer of **2** before and after rotation, and for the monomer of **2** using all of the basis functions of the dimer. We can thus investigate how the atomic charges change when the neighbouring cluster is taken away or when the -O*t*Bu group is rotated by about 60°.

Table 4. Mulliken and Roby–Davidson atomic charges [*e*] in one and two molecules of **2** as obtained from a TPSS/TZVPP population analysis, before (0°) and after (60°) rotation of the -O*t*Bu group.

	Mulliken				Roby–Davidson			
Rotation angle	0°		60°		0°		60°	
molecules of **2**	one	two	one	two	one	two	one	two
K(1b)	–	0.783	–	0.817	–	0.989	–	0.994
C(11)	−0.230	−0.262	−0.158	−0.159	−0.102	−0.105	−0.109	−0.112
C(12)	−0.187	−0.236	−0.136	−0.266	−0.113	−0.123	−0.104	−0.190
H(111)	0.053	0.064	0.048	0.053	0.031	0.030	0.040	0.037
H(112)	−0.001	−0.015	0.026	0.034	0.009	0.003	0.029	0.024
H(113)	0.040	0.046	0.035	0.037	0.025	0.022	0.018	0.010
H(121)	0.042	0.055	0.054	0.090	0.026	0.028	0.043	0.044
H(122)	0.037	0.045	0.058	0.015	0.028	0.024	0.038	0.003
H(123)	0.048	0.040	−0.029	0.023	0.035	0.020	0.004	0.028

In the dimer (not rotated), we find atomic charges on H(112) of −0.015 *e* (Mulliken) and 0.003 *e* (Roby–Davidson), which are significantly smaller than on the other H atoms listed in Table 4. Indeed, the atom H(112) is the H atom that is closest to the K atom of the neighbouring cluster. If we remove the neighbouring cluster, however, the atomic charges are still much smaller than those on the other hydrogen atoms.

After rotation by about 60°, the charge on H(122), which is now closest to K(1b), is the smallest atomic charge. Natural populations as computed by the NBO 5.G program are given in Table 5.

Table 5. NBO natural populations [*e*] in two molecules of **2** as obtained from a TPSS/6–31G** population analysis, before (0°) and after (60°) rotation of the -O*t*Bu group.

Rotation angle	0°	60°
K(1b)	0.921	0.917
C(11)	−0.694	−0.690
C(12)	−0.688	−0.707
H(111)	0.234	0.233
H(112)	0.204	0.219
H(113)	0.223	0.226
H(121)	0.239	0.228
H(122)	0.213	0.209
H(123)	0.215	0.218

Again we observe that the H···K(1b) distances correlate with the atomic charge on the hydrogen atoms. At 0°, H(112) has the smallest charge, at 60°, H(122) has the smallest charge. We observe some effects of the neighbouring cluster on the atomic charges, and some correlation between contact and charge, but the effects are small. Also the changes that occur when the *tert*-butoxy ligand is rotated by about 60° are small. Finally, the atomic charges, in particular the Roby–Davidson charges (+0.99 *e*), also provide strong evidence that the potassium is present in **2** as the cation K^+.

The computed K(1b)···H bond orders are perhaps the most interesting quantities for our analysis of the bonding electron density (Table 6). Although the bond orders are extremely small (they do not point at significant agostic interactions), we find again correlations between the K(1b)···H bond length and the computed property. The Wiberg bond indices are largest for the short K(1b)···H bonds (0.0018 and 0.0016 for H(112) and H(123), cf. Figure 4), and the same is true for the NAO bond orders (0.0100 and 0.0116, respectively). After rotation by about 60°, the K(1b)···H bonds are short for the atoms H(121), H(122) and H(123), and in this structure, these bonds show the largest bond orders. The computed bond orders correlate with the bond lengths, but we do not feel that the computed values hint at significant agostic interactions. On the contrary, the NBO analysis identifies the K(1b) atoms as an isolated molecular unit with doubly occupied 1s, 2s, 2p, 3s and 3p orbitals, that is, an atom without bonds. In the NBO analysis, it is present in **2** as a K^+ counterion.

Table 6. Wiberg bond indices and atom–atom overlap weighted NAO bond orders of the six K(1b)···H contacts between two molecules of **2** as obtained from a TPSS/6–31G** natural bond order analysis, before (0°) and after (60°) rotation of the -O*t*Bu group.

Rotation angle	0°		60°	
Bond order	Wiberg	NAO	Wiberg	NAO
H(111)	0.0001	−0.0006	0.0001	−0.0007
H(112)	0.0018	0.0100	0.0001	0.0004
H(113)	0.0008	0.0055	0.0001	0.0016
H(121)	0.0002	0.0002	0.0017	0.0113
H(122)	0.0010	0.0073	0.0028	0.0148
H(123)	0.0016	0.0116	0.0013	0.0074

The computational study of the high-spin Co^{II} clusters was partly performed to investigate the TPSS functional, which had been implemented recently in the TURBOMOLE program. On the compounds studied here, the performance of the modern TPSS functional was very similar to that of the popular B3LYP functional, but since the TPSS functional allowed us to use the (multipole-accelerated) RI-*J* approximation, the calculations with the TPSS functional were much faster than those with the B3LYP functional. Indeed the MARI-*J* approach was used in all of the calculations with the BP86 and TPSS functionals and allowed us to use the rather large TZVPP basis with 3636 contracted functions on the dimer of **2**.

Conclusion

Solvent-free alkali metal complexes can contain low-coordinate alkali metal atoms embedded in cavities formed by organic groups. Although C–CH_3···K distances found in the heterometallic alkoxide $[K_2Co_2(\mu_3\text{-}OtBu)_2(\mu_2\text{-}OtBu)_4]$ (**2**) are similar to short Si–CH_3···K distances observed in numerous compounds and often described as agostic interactions, a computational study has shown that in **2** close contacts are the result of steric requirements rather than of weak bonding interactions. Scherer and McGrady note in their recent and comprehensive review article on agostic interactions that such interactions have proved remarkably difficult to pin down and characterise in many alkyl systems.[20] For instance, these authors write: "Although the location of a hydrogen atom close to the metal center and the consequent reorganization of bonding electron density should result in major structural and spectroscopic changes in the M···HC moiety, characterization of the interaction is often fraught with difficulty." In the heterometallic alkoxide $[K_2Co_2(\mu_3\text{-}OtBu)_2(\mu_2\text{-}OtBu)_4]$ (**2**), we neither see major structural changes nor major changes in bonding electron density or atomic charges. Therefore, in this particular system, we fail to characterise the interaction as agostic. We believe that the DFT investigation of rotational barriers in *t*Bu or $SiMe_3$ groups of similar systems represents a useful tool to supplement calculations of atomic charges and bond orders for the theoretical analysis of weak metal···H···C interactions.

Experimental Section

All operations were carried out in an atmosphere of purified argon. Solvents were dried over sodium/benzophenone. Metal salts were purchased from Aldrich.

Preparation of 1–3: A solution of M*O*t*B*u (M = Na, K, Rb) (3.00 mmol) in THF (10 mL) was added to a solution of $CoBr_2$ (0.22 g, 1.00 mmol) in THF (10 mL). The solution was stirred at room temperature for 24 h. A colorless precipitate of MBr was filtered off. The solvent of the filtrate was removed under reduced pressure and the blue residue was dried under high vacuum for 1 h at room temperature. The solid was extracted with pentane (20 mL) and filtered. Concentration of the filtrate to about 3 mL and storage of the solution for two days produced blue crystals.

1: Yield 0.3 g, 80%; decomposition at 298°C into green solid; elemental analysis calcd (%) for $C_{28}H_{62}Co_2Na_2O_7$: C 49.8, H 9.2; found: C 49.7, H 9.1 (one thf ligand was removed during isolation); UV/Vis (thf): λ_{max} (ε): 511 (118), 601 (139), 684 (82) nm; IR (KBr): $\tilde{\nu}$ = 1201, 1094 (C–O), 475 (metal–O) cm^{-1}.

2: Yield 0.2 g, 63%; m.p. 260°C; elemental analysis calcd (%) for $C_{24}H_{54}Co_2K_2O_6 \cdot 0.5$ thf: C 46.6, H 8.7; found: C 46.9, H 8.7; UV/Vis (thf): λ_{max} (ε) = 510 (115), 610 (130), 670 (150) nm; IR (CsI, Nujol): $\tilde{\nu}$ = 1202, 1077, (C–O), 464, 398 (metal–O) cm^{-1}.

3: Yield 0.15 g, 57%; various color changes occur when solid samples are heated, 315°C green solid, 339°C blue solid; elemental analysis calcd (%) for $C_{24}H_{54}Co_2O_6Rb_2 \cdot 0.5$ thf (i.e. loss of 0.5 thf per $Rb_2\{Co_2(OtBu)_6\}$ entity): C 40.9, H 7.6; found: C 40.9, H 7.6; UV/Vis (thf): λ_{max} (ε): 503 (151), 604 (220), 670 (330) nm; IR (KBr): $\tilde{\nu}$ = 1195, 1003 (C–O), 490 (metal–O) cm^{-1}.

Crystallographic details: Data for **1** (Stoe STADI IV), **2** (Stoe IPDS I on a Schneider rotary anode X-ray generator), **3** and **3a** (Stoe IPDS II) were collected by using graphite-monochromated $Mo_{K\alpha}$ radiation (λ = 0.71073 Å). The structures were solved by direct methods and refined by full-matrix least-squares on F^2 (all data) using the SHELXTL program package.[21] Hydrogen atoms in **2** were located, and their coordinates refined; non-hydrogen atoms were assigned anisotropic thermal parameters. In **1** and **3** hydrogen atoms were placed in idealized positions. In the structure of **3**, the thf ligands are situated between the complex molecules, disordered over inversion centres. It was necessary to refine the carbon atoms with full-occupancy, and the oxygen atoms as half-occupancy atoms. Within a chain of molecules there is probably long-range order; but attempts to refine the structure in lower-symmetry space groups were unsuccessful, indicating that there is little or no ordering between the chains. In **3a** one heavily disordered molecule of THF is present per cluster. Because the solvent molecule could not be refined *squeeze* was applied.[22]

Crystal data for **1**: $C_{32}H_{70}Co_2Na_2O_8$; M_r = 746.72; orthorhombic, space group *Pbca*, Z = 4; a = 15.166(3), b = 15.301(3), c = 17.863(4) Å; V = 4145.2(14) $Å^3$; T = 200(2) K; $F(000)$ = 1608; ρ_{calcd} = 1.197 $g\,cm^{-3}$. A total of 26890 reflections measured, of which 5441 were unique (R_{int} = 0.0379); 199 parameters; final wR_2 = 0.1311 (all data); R_1 = 0.0411 {$I > 2\sigma(I)$}; largest difference peak and hole 0.884 and −0.405 $eÅ^{-3}$.

Crystal data for **2**: $C_{24}H_{54}Co_2K_2O_6$; M_r = 634.73; triclinic, space group $P\bar{1}$, Z = 1; a = 9.9044(12), b = 10.0457(13), c = 10.2887(13) Å, α = 61.879(13), β = 65.459(13), γ = 80.717(15)°; V = 820.53(18) $Å^3$; T = 203(2) K; $F(000)$ = 338; ρ_{calcd} = 1.285 $g\,cm^{-3}$. A total of 5322 reflections measured, of which 2954 were unique (R_{int} = 0.0297); 235 parameters; final wR_2 = 0.0777 (all data); R_1 = 0.0297 {$I > 2\sigma(I)$}; largest difference peak and hole 0.310 and −0.333 $eÅ^{-3}$.

Crystal data for **3**: $C_{28}H_{62}Co_2O_7Rb_2$; M_r = 799.58; monoclinic, space group $P2_1/n$, Z = 1; a = 10.837(2), b = 12.684(3), c = 13.937(3) Å, β = 93.55(3)°; V = 1912.0(7) $Å^3$; T = 150(2) K; $F(000)$ = 828; ρ_{calcd} = 3.432 $g\,cm^{-3}$. A total of 4775 reflections measured, of which 2720 were unique (R_{int} = 0.0473); 179 parameters; final wR_2 = 0.1319 (all data); R_1 = 0.0522 {$I > 2\sigma(I)$}; largest difference peak and hole 0.679 and −0.507 $eÅ^{-3}$.

Crystal data for **3a**: $C_{28}H_{62}Co_2O_7Rb_2$; M_r = 799.58; monoclinic, space group $C2/m$, Z = 2; a = 16.993(3), b = 12.8646(15), c = 10.873(2) Å, β = 126.250(13)°; V = 1916.9(5) $Å^3$; T = 100(2) K; $F(000)$ = 828; ρ_{calcd} = 3.423 $g\,cm^{-3}$. A total of 6325 reflections measured, of which 2344 were unique (R_{int} = 0.0691); 82 parameters; final wR_2 = 0.2221 (all data); R_1 = 0.0754 {$I > 2\sigma(I)$}; largest difference peak and hole 0.975 and −0.969 $eÅ^{-3}$.

CCDC-285839–CCDC-285842 contain the supplementary crystallographic data for this paper. These data can be obtained free of charge from The Cambridge Crystallographic Data Centre via www.ccdc.cam.ac.uk/data_request/cif.

Acknowledgements

The authors thank the DFG Research Center for Functional Nanostructures (CFN, project number C3.3) and the Forschungszentrum Karlsruhe (A. R.) for financial support. The authors thank A. Daniel Boese for providing them with the NBO analysis from TPSS/6–31G** calculations with the Gaussian 03 program at the Weizmann Institute (Rehovot, Israel). A. R. thanks Prof. D. Fenske for his support.

[1] a) S. Osa, Y. Sunatsuki, Y. Yamamoto, M. Nakamura, T. Shimamoto, N. Matsumoto, N. Re, *Inorg. Chem.* **2003**, *42*, 5507; b) M. Murrie, S. J. Teat, H. Stoeckli-Evans, H. U. Gudel, *Angew. Chem.* **2003**, *115*, 4801; *Angew. Chem. Int. Ed.* **2003**, *42*, 4653; c) G. Aromi, A. S. Batsanov, P. Christian, M. Helliwell, A. Parkin, S. Parsons, A. A. Smith, G. A. Timco, R. E. P. Winpenny, *Chem. Eur. J.* **2003**, *9*, 5142.

[2] M. Bochmann, G. Wilkinson, G. B. Young, M. B. Hursthouse, K. M. A. Malik, *J. Chem. Soc. Dalton Trans.* **1980**, 901.

[3] G. A. Sigel, R. A. Bartlett, D. Decker, M. M. Olmstead, P. P. Power, *Inorg. Chem.* **1987**, *26*, 1773.

[4] D. C. Bradley, R. C Mehrotra, D. P. Gaur, *Metal Alkoxides*, Academic Press, New York **1978**.

[5] M. M. Olmstead, P. P. Power, G. Siegel, *Inorg. Chem.* **1986**, *25*, 1027.

[6] G. C. Forbes, A. R. Kennedy, R. E. Mulvey, B. A. Roberts, R. B. Rowlings, *Organometallics* **2002**, *21*, 5115, and references therein.

[7] K. W. Klinkhammer, *Chem. Eur. J.* **1997**, *3*, 1418.

[8] M. Moore, S. Gambarotta, C. Bensimon, *Organometallics* **1997**, *16*, 1086.

[9] F. Feil, S. Harder, *Organometallics* **2000**, *19*, 5010.

[10] a) M. Brookhart, M. L. H. Green, L.-L. Wong, *Prog. Inorg. Chem.* **1988**, *36*, 1; b) R. H. Crabtree, D. G. Hamilton, *Adv. Organomet. Chem.* **1988**, *28*, 299; c) R. H. Crabtree, *Angew. Chem.* **1993**, *105*, 828; *Angew. Chem. Int. Ed. Engl.* **1993**, *32*, 789; d) W. Baratta, C. Mealli, E. Herdtweck, A. Ienco, S. A. Mason, P. Rigo, *J. Am. Chem. Soc.* **2004**, *126*, 5549, and references therein.

[11] L. Ponikiewski, A. Rothenberger, *Inorg. Chim. Acta* **2005**, *358*, 1322.

[12] A. P. Purdy, C. F. George, *Polyhedron* **1994**, *13*, 709.

[13] Y. K. Gun′ko, U. Christmann, V. G. Kessler, *Eur. J. Inorg. Chem.* **2002**, 1029.

[14] T. J. Woodman, M. Schormann, D. L. Hughes, M. Bochmann, *Organometallics* **2003**, *22*, 3028.

[15] All calculations were performed with the TURBOMOLE program package. a) R. Ahlrichs, M. Bär, M. Häser, H. Horn, C. Kölmel, *Chem. Phys. Lett.* **1989**, *162*, 165; b) O. Treutler, R. Ahlrichs, *J. Chem. Phys.* **1995**, *102*, 346. Results are reported that were obtained with the TPSS exchange-correlation functional within the multipole-accelerated resolution-of-the-identity (MARI-*J*) approximation. c) J. Tao, J. P. Perdew, V. N. Staroverov, G. E. Scuseria, *Phys. Rev. Lett.* **2003**, *91*, 146401; d) K. Eichkorn, O. Treutler, H. Öhm, M. Häser, R. Ahlrichs, *Chem. Phys. Lett.* **1995**, *240*, 283; K. Eichkorn, O. Treutler, H. Öhm, M. Häser, R. Ahlrichs, *Chem. Phys. Lett.* **1995**, *242*, 652; e) M. Sierka, A. Hogekamp, R. Ahlrichs, *J. Chem. Phys.* **2003**, *118*, 9136. The TZVPP basis with corresponding auxiliary basis set was used as available in the TURBOMOLE basis-set library.

[16] a) E. R. Davidson, *J. Chem. Phys.* **1967**, *46*, 3320; b) K. R. Roby, *Mol. Phys.* **1974**, *27*, 81.

[17] C. Ehrhardt, R. Ahlrichs, *Theor. Chim. Acta* **1985**, *68*, 231.

[18] Gaussian 03, Revision C.01wis5, (WIS customized version 5) see intranet http://harriet.weizmann.ac.il/g~03wis.html for documentation of additional features. M. J. Frisch, G. W. Trucks, H. B. Schlegel, G. E. Scuseria, M. A. Robb, J. R. Cheeseman, J. A. Montgomery, Jr., T. Vreven, K. N. Kudin, J. C. Burant, J. M. Millam, S. S. Iyengar, J. Tomasi, V. Barone, B. Mennucci, M. Cossi, G. Scalmani, N. Rega, G. A. Petersson, H. Nakatsuji, M. Hada, M. Ehara, K. Toyota, R. Fukuda, J. Hasegawa, M. Ishida, T. Nakajima, Y. Honda, O. Kitao, H. Nakai, M. Klene, X. Li, J. E. Knox, H. P. Hratchian, J. B. Cross, C. Adamo, J. Jaramillo, R. Gomperts, R. E. Stratmann, O. Yazyev, A. J. Austin, R. Cammi, C. Pomelli, J. W. Ochterski, P. Y. Ayala, K. Morokuma, G. A. Voth, P. Salvador, J. J. Dannenberg, V. G. Zakrzewski, S. Dapprich, A. D. Daniels, M. C. Strain, O. Farkas, D. K. Malick, A. D. Rabuck, K. Raghavachari, J. B. Foresman, J. V. Ortiz, Q. Cui, A. G. Baboul, S. Clifford, J. Cioslowski, B. B. Stefanov, G. Liu, A. Liashenko, P. Piskorz, I. Komaromi, R. L. Martin, D. J. Fox, T. Keith, M. A. Al-Laham, C. Y. Peng, A. Nanayakkara, M. Challacombe, P. M. W. Gill, B. Johnson, W. Chen, M. W. Wong, C. Gonzalez, and J. A. Pople, Gaussian, Inc., Wallingford CT, **2004**.

[19] NBO 5. G. E. D. Glendening, J. K. Badenhoop, A. E. Reed, J. E. Carpenter, J. A. Bohmann, C. M. Morales, and F. Weinhold (Theoretical Chemistry Institute, University of Wisconsin, Madison, WI, **2001**); http://www.chem.wisc.edu/~nbo5.

[20] W. Scherer, G. S. McGrady, *Angew. Chem.* **2004**, *116*, 1816; *Angew. Chem. Int. Ed.* **2004**, *43*, 1782.

[21] SHELXTL-97, G. M. Sheldrick, University of Göttingen, **1997**.

[22] A. L. Spek, *J. Appl. Crystallogr.* **2003**, *36*, 7.

Received: May 30, 2005
Revised: October 14, 2005
Published online: December 21, 2005

